Available online at www.sciencedirect.com
ScienceDirect
Medical Laser Application 26 (2011) 67–75
Medical Laser Application
www.elsevier.de/mla

Cutting effects induced by 2 μm laser radiation of cw Tm:YLF and cw and Q-switched Ho:YAG lasers on *ex-vivo* tissue

Oleg L. Antipov[a,*], Nikita G. Zakharov[a], Michael Fedorov[b], Natalia M. Shakhova[a,c], Natalia N. Prodanets[c], Ludmila B. Snopova[c], Valerij V. Sharkov[a,d], Ronald Sroka[b]

[a]*Institute of Applied Physics (IAP) of the Russian Academy of Science (RAS), 46 Ulyanov Street, 603950 Nizhny Novgorod, Russia*
[b]*Laser-Research Laboratory, LIFE Center, Ludwig Maximilians University, Großhadern Medical Campus, Marchioninistr. 23, 81377 Munich, Germany*
[c]*Nizhny Novgorod Medical Academy, 10/1 Minin Square, 603005 Nizhny Novgorod, Russia*
[d]*Nizhny Novgorod State University, 23 Gagarin Avenue, 603950 Nizhny Novgorod, Russia*

Received 8 October 2010; accepted 3 February 2011

Abstract

Background and objectives: Laser radiation in the 2 μm wavelength region is well-absorbed by water and has good transmittance through commercially available, low-OH quartz optical fibers which are generally acknowledged to have great potential for medical application in endoscopic and open surgery. Medical laser systems in this wavelength range are flashlamp- or laser-pumped pulsed Ho:YAG lasers and continuous wave (cw) thulium (Tm)-doped fiber lasers. This paper presents the laser–tissue effects on an *ex-vivo* tissue model using an innovative diode-pumped cw Tm:YLF laser and cw and Q-switched Ho:YAG laser.

Materials and methods: The diode-pumped air-cooled Tm:YLF laser (IAP RAS prototype) emits cw light at 1909 nm with an output power of up to 20 W and an optic-to-optic efficiency of more than 41%. The Ho:YAG laser (IAP RAS prototype) is pumped by the radiation of a Tm:YLF laser and can operate at 2090 nm in cw or Q-switched mode with an average power of up to 10 W. The laser beam quality of both lasers is about $M^2 < 1.3$ and can be easily coupled in low-OH optical fibers.

Laser–tissue interaction experiments were performed using porcine kidney and liver tissue. Single-spot and cutting experiments were performed in a reproducible set-up. In the single-spot experiments, a fixed distance was used between fiber and tissue surface of $d = 5$ mm and energies were applied in the 10–200 J range. The cutting experiments were performed with the same laser parameters but in contact mode ($d = 0$ mm) using a constant scanning velocity of $v = 1$ mm/s of the linear fiber movement. Macroscopic and histological evaluations were performed.

Results: The tissue effect showed precise and reproducible ablation. The ablation depth depended on the applied power. Interestingly, the histological findings showed that the thickness of the coagulation zone in lateral and axial plane was nearly constant at 1 ± 0.5 mm in each direction.

Conclusion: The presented lasers showed more flexibility for surgical approaches. The induced tissue effects showed a very high reproducibility in ablation and in coagulation for both radial and axial planes. The constant small size of these effects may show the potential for precise laser-assisted surgical preparation.

Keywords: Laser surgery; Infrared laser; 2 μm wavelength range; Laser–tissue interaction; Tm- and Ho-doped laser crystals

*Corresponding author. Tel.: +7 903 8463849; fax: +7 831 4363792.
E-mail address: antipov@appl.sci-nnov.ru (O.L. Antipov).

1615-1615/$ – see front matter © 2011 Published by Elsevier GmbH.
doi:10.1016/j.mla.2011.02.004

Introduction

Laser radiation with a wavelength of 2 μm is well-absorbed by water but still has good transmittance through commercially available optical low-OH quartz fibers [1–3]. From the medical point of view, application of this laser wavelength to tissue seems to be a good compromise between precise cutting, low thermal damage and sufficient coagulation for hemostasis [4,5]. Lasers with these properties have the potential of being used in diverse medical surgical applications, either directly or using the endoscopic approach in several medical disciplines such as urology, gynecology and cardiology. Up to now, medical approved laser devices emitting at this wavelength have been technically based on the flashlamp-pumped pulsed holmium:yttrium–aluminum–garnet (Ho:YAG) laser (λ = 2100 nm), and on the relatively new continuous wave (cw) emitting thulium (Tm)-fiber laser or diode-pumped thulium:yttrium–aluminum–garnet (Tm:YAG) laser with emission wavelengths in the range of 1900–2014 nm. However, due to the physical generation of the laser light, the flashlamp-pumped Ho:YAG laser can operate only in pulsed modes with a low repetition rate whereas the Tm-fiber laser or diode-pumped Tm:YAG laser generates cw radiation [5–9].

This paper presents two experimental innovative laser systems: (1) a diode-pumped cw thulium-doped yttrium lithium fluoride (Tm:YLF) laser emitting at a wavelength of λ = 1909 nm and (2) a laser-pumped Ho:YAG laser emitting light at a wavelength of λ = 2090 nm either in Q-switched or in cw mode. Both lasers were used to investigate their potential with respect to cutting and coagulation on an *ex-vivo* tissue model.

Materials and methods

Two different 2 μm lasers based on Tm:YLF and Ho:YAG crystals were developed at the Institute of Applied Physics (IAP) of the Russian Academy of Science (RAS) and optimized for experimental use in *ex-vivo* surgery trials on model tissue.

Tm:YLF laser

The prototype of the diode laser-pumped Tm:YLF laser (IAP RAS, Russia) consists of a Tm:YLF rod, longitudinally and simultaneously pumped from the opposite ends by two fiber-coupled diode laser bars at λ = 792 nm (Coherent GmbH, Germany; optical output power up to 45 W) as shown in Fig. 1. The laser elements and the cavity were optimized to obtain the maximum output power and high conversion efficiency [10].

The pumping beam diameter was optimized by a telescope optic to achieve a high-power generation beam without damaging the rod surfaces. In this way the pump beam could be directly fed into the Tm:YLF crystal. The laser cavity was configured by a plane, highly reflective mirror (λ = 1909 nm) and an output coupler designed as concave mirror with a reflectivity varying from 80 to 89%. For optimization, the radius of the output coupler mirror varied from 200 to 300 mm and the physical resonator length varied from 5 to 25 cm by moving the output coupler to achieve the best overlap of the pumping beam and the laser beam inside the laser rod. During the optimization process a maximum output power could be achieved using a cavity length of 14 cm and an output coupler with a reflection of 89% and a radius of 300 mm.

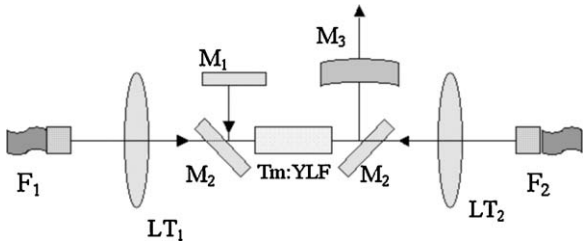

Fig. 1. Schematic set-up of the Tm:YLF laser. F_1 and F_2 are fiber outputs of the fiber-coupled diode lasers, LT_1 and LT_2 are lensed telescopes, M_1 is the high-reflection mirror, M_2 are transparent mirrors for the pumping beam and reflective mirrors for the generation beam, and M_3 is the output coupler [10].

Assuming an increase in up-conversion population of the upper laser level, which is necessary for Tm:YLF lasing and to reduce heat deposition via non-radiative decay, several crystal rods containing different Tm^{3+} concentrations (2.5 at.% < c(Tm^{3+}) < 3.5 at.%) were tested to maximize the laser output power. Furthermore, different Tm:YLF rod sizes were also tested to increase the output power. The optimization process deals with rod diameters varying from 2 to 5 mm, and rod lengths varying from 10 to 18 mm, each with a cut surface and antireflection-coated end faces for pumping at λ = 792 nm and lasing at λ = 1909 nm. The Tm:YLF rods have a different length for each Tm-doping concentration.

As a result of the optimization process, a laser emitting light was created in the cw mode at λ = 1909 nm with a maximum output power of 31 W. The slope efficiency for the output power was >50% and the optical efficiency was 47% (with respect to the total pump power fed into the rod). The transverse distribution of laser beam intensity was registered using infrared (IR) camera techniques (Pyrocam III; Spiricon GmbH, Germany). The measured quality of the output beam was determined by ISO test method [11] at a power of 30 W with an M^2-parameter of less than 1.3. The small divergence of the laser radiation offers a good opportunity for efficient coupling of the laser light into optical fibers. This laser system could run efficiently with only fan cooling instead of water cooling.

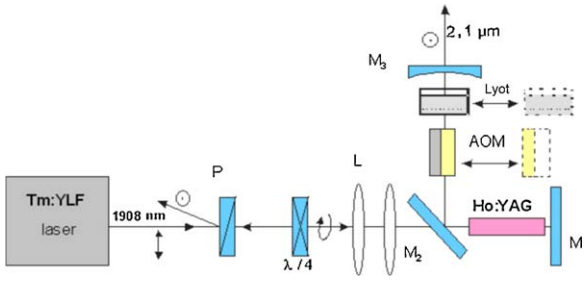

Fig. 2. The schematic set-up of the Ho:YAG laser pumped by the Tm:YLF laser with P as a polarizer, λ/4 is a quarter wavelength plate, M is the mirror, L is a lens, AOM is the acousto-optical modulator and Lyot is the filter [12].

Ho:YAG laser

The innovative Ho:YAG laser (IAP RAS, Russia) is pumped by the radiation of the Tm:YLF laser as shown in Fig. 2 [12]. The active rod of the Ho:YAG laser was 25 mm in length with an undoped, diffusion bonded end cap. The laser cavity was formed by a flat mirror with high reflectivity, a flat 45° dichroic mirror with high reflectivity at the wavelength of $\lambda = 2090$ nm and a high transmission at the pump wavelength of $\lambda = 1909$ nm, together with a concave output coupler. To obtain maximum output power, the pump beam diameter inside the active element was expanded in the range of 0.53–0.8 mm; the output-coupler curvature varied from 150 to 300 mm. The physical resonator length varied during the optimization process from 5 to 25 cm.

In this way the Tm:YLF laser pumped the Ho:YAG laser, emitting light with the average laser power of up to 10 W in the cw and Q-switched mode. The optic-to-optic efficiency reached values of >55%. The introduction of a silica acousto-optic modulator (AOM) in front of the output coupler changed the cw system into a pulsed Q-switched laser emitting laser pulses of pulse durations of 25–100 ns at tunable repetition rates between 3 and 15 kHz resulting in peak powers of 125 kW and 25 kW, respectively. Single spectral laser lines could be selected using an intracavity 2-plate birefringent filter (Lyot filter) coupled to the tuning element. This allowed the individual spectral wavelengths 2090, 2097 and 2123 nm to be generated in cw as well as in the Q-switched mode. The output power at $\lambda = 2090$ nm of the Ho:YAG laser was decreased by the intracavity selector by less than 2% in comparison with the selector-free laser. The Ho:YAG-laser beam showed a good beam quality with an M^2-parameter of less than 1.3, which was recorded with IR camera techniques (Pyrocam III; Spiricon GmbH, Germany) and determined by the ISO test method [11]. Therefore the Ho:YAG laser light could be fed into optical low-OH fibers very well. Using this laser set-up, IR light emission was generated in cw or Q-switched modes with pulse durations of 25–100 ns, or hundreds of microseconds (μs) to hundreds of milliseconds (ms).

Ex-vivo experiments

Fresh porcine liver and kidney were used as the *ex-vivo* tissue model. For the experiments the laser radiation was transferred from the laser to the tissue via a low-OH flat-cut, bare-ended optical fiber with a core diameter of 600 μm. The fiber end was positioned perpendicular to the tissue surface, either in non-contact (single-spot experiments) or in contact (cutting experiments) according to different potential clinical approaches.

Laser applications were performed using only fan cooling. The laser power at the distal fiber end was measured before each experiment in order to verify the stability of the laser emission. The experimental laser parameters used are listed in Table 1.

The single-spot experiments were performed with a constant fiber-to-tissue surface distance of $d = 5$ mm. The Ho:YAG laser was run (1) in cw with its maximum output power of 10 W and application times of 1, 5, and 10 s, or (2) in the Q-switched mode at repetition rates of 3, 8 and 15 kHz at the same output power of 10 W and an application time of 10 s (Table 1). The Tm:YLF laser was set to 10 W and also to its maximum output power of 20 W using the same application times as for the Ho:YAG laser (Table 1). Each experiment was performed five times on both types of tissue. Macroscopically, the ablation depth, the axial coagulation depth and the width of the radial coagulation edge were measured by the use of calipers.

The same laser parameters were used for the cutting experiments as for the single-spot experiments (Table 1) but the experiments were performed by positioning the fiber end in smooth contact ($d = 0$ mm) to the tissue surface. The fiber was fixed in a holder which was coupled to a computer-driven stepping motor enabling to move the fiber linear over the tissue surface with a constant velocity of 1 mm/s over a cutting length of 4 cm. Three cutting lines were created in this way. For evaluation purposes, the tissue was cut perpendicular to the cut at 1, 2 and 3 cm of the cutting line. Macroscopically, the ablation depth, the axial coagulation depth and the width of the radial coagulation edge were measured using calipers.

Histology

Tissue samples were harvested for morphological verification of the laser-induced effects. Cryotome tissue sections (10–15 μm) were made, stained with hematoxylin and eosin (H&E) and subjected to histological assessment with light microscopy (Leica DM 1000; Leica Microsystems, Germany).

Evaluation and statistics

For each set of laser parameters, mean and standard deviations (SDs) of the measured data (ablation depth, axial coagulation depth and width of the radial coagulation edge)

Table 1. Parameters of the lasers used in the single-spot and cutting experiments.

Laser type	Wavelength (nm)	Emission mode	Average laser power (W)	Application time (s)	Pulse repetition rate (kHz)	Pulse duration (ns)	Applied energy (J)
Ho:YAG	~2090	cw	10	1			10
				5			50
				10			100
Ho:YAG	~2090	Q-switched	10	10	3	25–30	100
					8	45–50	
					15	90–100	
Tm:YLF	~1909	cw	10	1			10
				5			50
				10			100
			20	1			20
				5			100
				10			200

were calculated from the repeated measurements. Statistical evaluation (Student's *t*-test) was made and diagrams were prepared using scientific standard software (SigmaPlot v11; Jandel Scientific Corp., USA). The significance level was set at 5% ($p = 0.05$).

Results

Immediate tissue effects could be observed showing superficial coagulation, carbonization, vaporization and ablation.

Single-spot experiments

In Figs. 3 and 4 the single-spot experiments on liver and kidney show an increase in the ablation depth with respect to the applied energy, while both the coagulation edge and the axial coagulation depth are approximate, and remain constant in the range of 1 mm. The results show that the tissue effects on the liver are slightly greater than on that of the kidney tissue, and the Ho:YAG laser induces larger tissue effects compared to the Tm:YLF laser. In the case of the Tm:YLF laser, the increase of the laser power to 20 W, thus increasing the applied energy up to 200 J, induced an increase in the ablation depth, whereas the coagulation effects remain in the range of 1 mm as shown in Figs. 5 and 6. Changing from the Ho:YAG cw mode to the Ho:YAG Q-switched mode, using the same average power and total applied energy, the ablation depth remains constant at a level of 5 mm for liver tissue compared to 4 mm for kidney tissue, as is shown in Figs. 7 and 8. Here also the coagulation values are approximately 1 mm in the axial plane as well as in the radial plane for both tissues.

Statistical analysis of the single-spot experiments showed no significant difference ($p > 0.05$) between the values for the radial coagulation edge and the axial coagulation depth

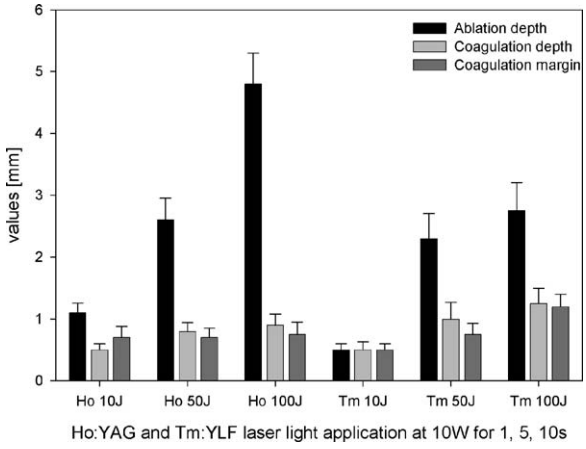

Fig. 3. Single-spot experiments (fiber–tissue distance $d = 5$ mm) on porcine liver tissue using Ho:YAG and Tm:YLF laser in cw mode ($P = 10$ W, $t = 1$, 5, and 10 s). Mean and standard deviations of ablation depth, axial coagulation depth and width of the radial coagulation edge are shown.

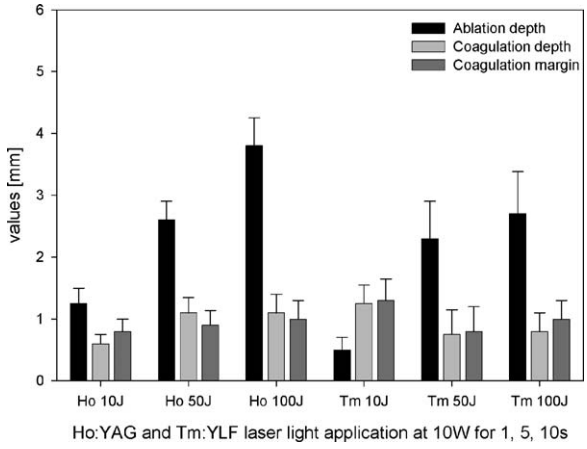

Fig. 4. Single-spot experiments (fiber–tissue distance $d = 5$ mm) on porcine kidney tissue using Ho:YAG and Tm:YLF laser in cw mode ($P = 10$ W, $t = 1$, 5, and 10 s). Mean and standard deviations of ablation depth, axial coagulation depth and width of the radial coagulation edge are shown.

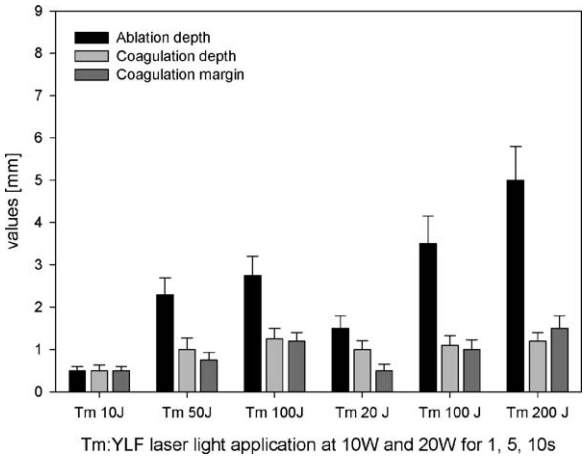

Fig. 5. Single-spot experiments (fiber–tissue distance $d = 5$ mm) on porcine liver tissue using Tm:YLF laser in cw mode ($P = 10$ and 20 W, $t = 1$, 5, and 10 s). Mean and standard deviations of ablation depth, axial coagulation depth and width of the radial coagulation edge are shown.

comparing the different laser types (Ho:YAG vs. Tm:YLF laser) and the induced effects on both tissue types (liver vs. kidney). The only statistical significance ($p < 0.05$) that could be evaluated was for the ablation depth in terms of both the laser types used, and the different tissue types.

Cutting experiments

The induced tissue effects after the cutting experiments (Figs. 9 and 10) showed that there is only a slight variation in the ablation depth when the average laser power was set to 10 W in the different laser emission modes, but an increased ablation effect when 20 W was used. It is of note that the

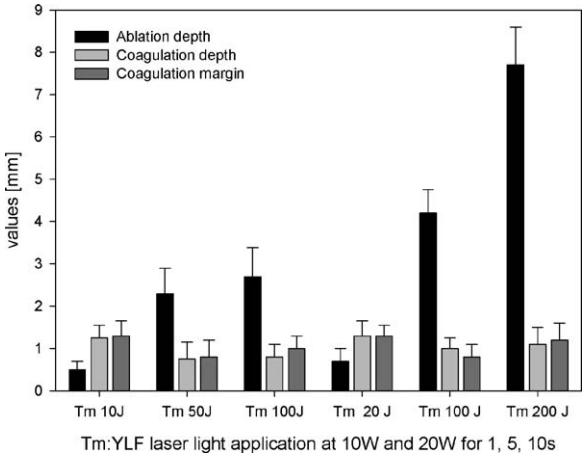

Fig. 6. Single-spot experiments (fiber–tissue distance $d = 5$ mm) on porcine kidney tissue using Tm:YLF laser in cw mode ($P = 10$ W and 20 W, $t = 1$, 5, and 10 s). Mean and standard deviations of ablation depth, axial coagulation depth and width of the radial coagulation edge are shown.

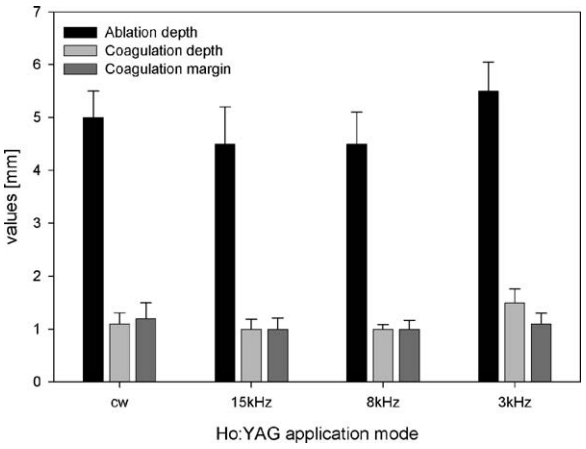

Fig. 7. Single-spot experiments (fiber–tissue distance $d = 5$ mm) on porcine liver tissue using the Ho:YAG laser either in cw or in Q-switched mode at repetition rates of 15, 8 and 3 kHz ($P = 10$ W, $t = 10$ s) resulting in a total applied energy of 100 J for all experiments. Mean and standard deviations of ablation depth, axial coagulation depth and width of the radial coagulation edge are shown.

mean coagulation in the radial as well as in the axial plane was about 1 mm for each set of experimental parameters.

Statistical analysis of the cutting experiments showed no significant difference ($p > 0.05$) between the radial coagulation edge and the axial coagulation. No significant differences could be evaluated when comparing these values with respect to the tissues ($p > 0.05$), which was also the case for the ablation depth. Regarding the different laser types, both the Ho:YAG (cw/Q-switched) and the cw Tm:YLF induced similar coagulation edges (Tm:YLF 20 W was excluded from statistical evaluation).

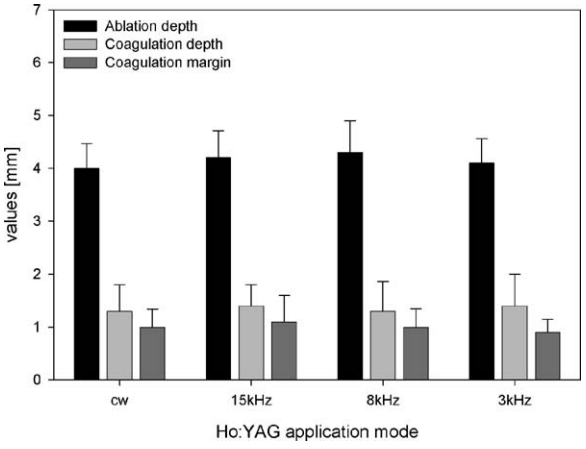

Fig. 8. Single-spot experiments (fiber–tissue distance $d = 5$ mm) on porcine kidney tissue using the Ho:YAG laser either in cw or in Q-switched mode at repetition rates of 15, 8 and 3 kHz ($P = 10$ W, $t = 10$ s) resulting in a total applied energy of 100 J for all experiments. Mean and standard deviations of ablation depth, axial coagulation depth and width of the radial coagulation edge are shown.

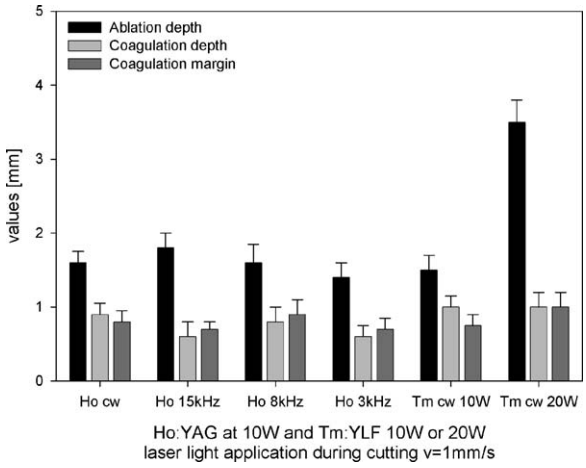

Fig. 9. Cutting experiments (fiber–tissue distance $d = 0$ mm, scanning velocity $v = 1$ mm/s) on porcine liver tissue using the Ho:YAG laser either in cw or in Q-switched mode at repetition rates of 15, 8 and 3 kHz ($P = 10$ W, $t = 10$ s) resulting in a total applied energy of 100 J and the Tm:YLF laser in cw mode at an output power of 10 W and 20 W resulting in a total applied energy of 100 and 200 J respectively. Mean and standard deviations of ablation depth, axial coagulation depth and width of the radial coagulation edge are shown.

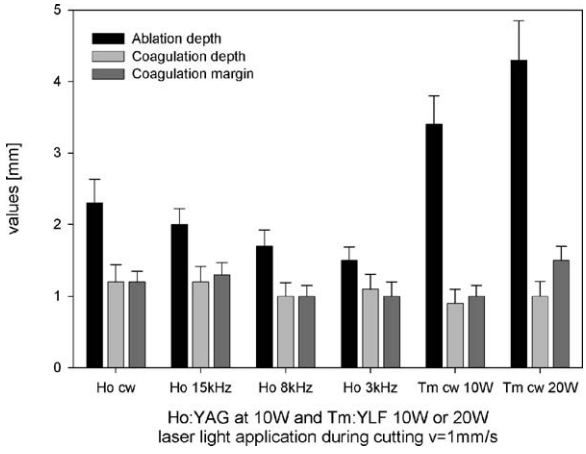

Fig. 10. Cutting experiments (fiber–tissue distance $d = 0$ mm, scanning velocity $v = 1$ mm/s) on porcine kidney tissue using the Ho:YAG laser either in cw or in Q-switched mode at repetition rates of 15, 8 and 3 kHz ($P = 10$ W, $t = 10$ s) resulting in a total applied energy of 100 J and the Tm:YLF laser in cw mode at an output power of 10 W and 20 W resulting in a total applied energy of 100 and 200 J respectively. Mean and standard deviations of ablation depth, axial coagulation depth and width of the radial coagulation edge are shown.

Histological evaluation

Fig. 11 shows an example of the H&E stained lateral section of kidney induced by cw Ho:YAG laser irradiation after single spot-application of 50 J ($P = 10$ W, $t = 5$ s). The crater surface showed minor signs of carbonization whereas in the surrounding tissue coagulation and vacuolization effects can

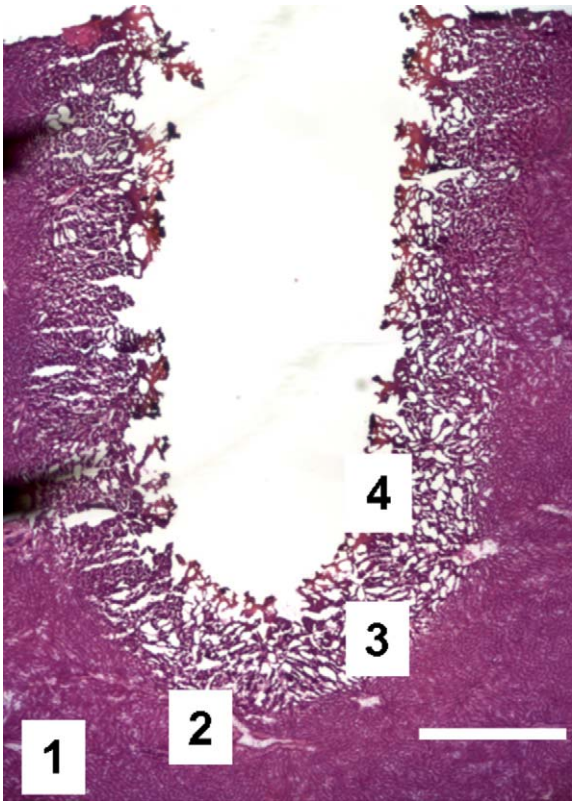

Fig. 11. Lateral section of H&E stained porcine kidney tissue crater induced by cw Ho:YAG laser irradiation after single spot-application of 50 J ($P = 10$ W, $t = 5$ s). The slide shows the effects on the remaining tissue as indexed "1" normal, i.e. thermal unaffected tissue, "2" heat-affected tissue, "3" coagulated tissue showing vacuolization, and "4" signs of carbonized tissue (bar: 1 mm).

be observed due to the thermal impact. This slide shows that the surrounding tissue of the crater was thermally affected both radially and axially to a similar degree, i.e. 1 mm.

Minor differences in the radial tissue response due to different repetition rates of Q-switched Ho:YAG laser application are shown in Fig. 12 compared to cw laser light-induced effects. It could be deduced from these slides that the occurrence of carbonization increased at lower repetition rates and cw application. In the same way the occurrence of thermal coagulation and vacuolization changed.

Discussion

An innovative fan cooled laser system in the 2 μm wavelength regime was designed for laboratory experiments. The complete laser system could be realized in a modular manner, which allowed the use of the pumping beam of the Tm:YLF laser as an independent, useable laser with a wavelength of 1909 nm. The Ho:YAG laser could be switched in the wavelength range of 2090–2123 nm and in two different emitting modes (cw or Q-switched). Further experiments using the different possible laser parameters are needed to identify the

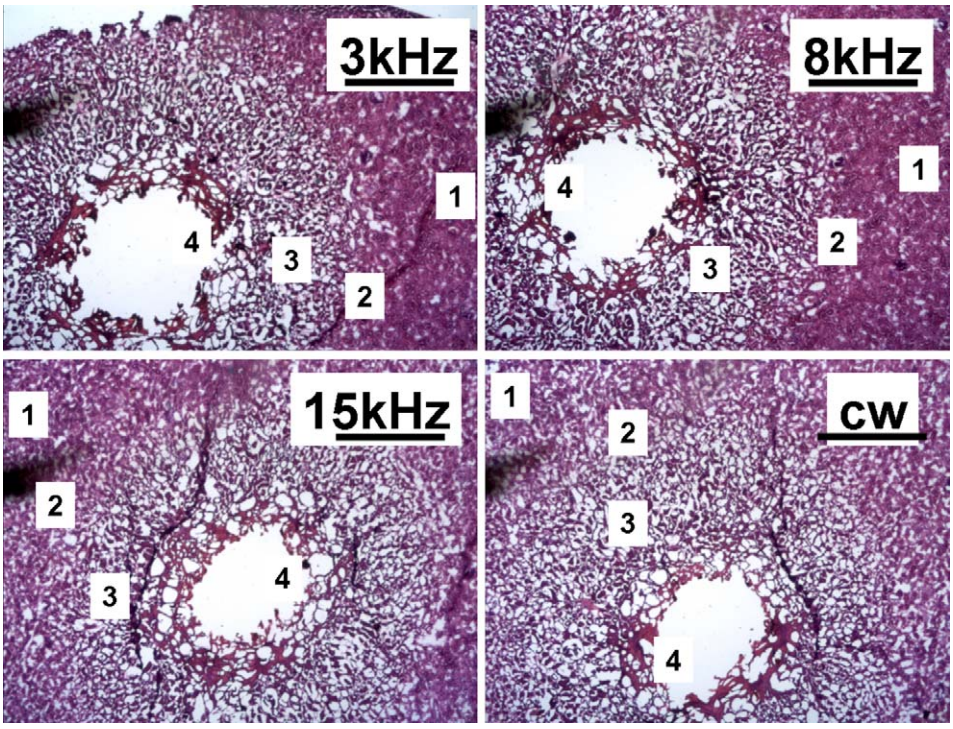

Fig. 12. Cross section of H&E stained porcine kidney tissue of Q-switched Ho:YAG laser-induced crater after single-spot application of 100 J using different repetition rates of 3, 8 and 15 kHz at the same average power ($P = 10$ W) as in comparison to the cw Ho:YAG laser light application. The slide shows the radial effects on the remaining tissue as indexed "1" normal, i.e. thermal unaffected tissue, "2" heat-affected tissue, "3" coagulated tissue showing vacuolization, and "4" signs of carbonized tissue (bar: 1 mm).

clinical uses that the technical possibilities of this laser system have to offer. Overall the maximum output power from the existing system of 10 W for the Ho:YAG and 20 W for the Tm:YLF must be increased.

In this preliminary investigation, the tissue effects of a couple of laser parameters were shown on two different tissue models. Overall, all used lasers showed efficient tissue ablation as well as coagulation. The ablation depth differed with respect to the tissue and with increasing applied energy. As these effects depend on the specific optical and thermal tissue parameters, it is of interest that especially the coagulation in axial and radial direction showed comparable sizes without any significant differences. Thus the affected remaining tissue showed the same degree of thermal damage in both the lateral and the axial planes.

These macroscopic findings can be explained by taking the thermal and optical properties of the tissue models into account. As the thermal conductivity and the heat capacity of the model tissues are nearly the same [13] the heat transport either in radial or in axial direction follows the same decline thus resulting in comparable tissue temperatures and effects. Unfortunately optical properties in the spectral region near to 2000 nm are not available for the model tissues. Theoretically, in this spectral region the scattering coefficient μ_s differs marginally. As the model tissues contain about the same amount of water [13], the absorption coefficient of water can be taken into account. At 1909 nm a μ_a of about 12 mm^{-1} and at 2090 nm a value of 3 mm^{-1} can be derived from the water absorption curve [14]. Temperature-induced tissue effects based on such marginal differences could only be verified by further experiments and additional histological examinations. Furthermore, as the applied energy of the different application modes exceeded the ablation threshold of the tissue and the thermal properties of the tissues are about the same, a macroscopic significance in the thickness of the coagulation margins could not be derived.

Should there be precise defined coagulation in both the lateral and in the axial planes, something which must be verified in further *ex-vivo* and *in-vivo* experiments, this laser system could show considerable potential for use as a surgical preparation tool. On the other hand it must also be shown in *ex-vivo* perfused tissue models whether or not the induced coagulation is sufficient to seal small and larger vessels alike. While the macroscopic effects show high reproducibility, the microscopic observed effects such as vacuolization and the dependency on different repetition rates must be further investigated.

From the clinical point of view there are currently some laser systems clinically available which emit in the 2 μm spectral region with high output powers [15–18]. Unfortunately these systems do not allow either the wavelength or the emission mode to be changed. Furthermore, the emission lines do not fit the maximum of water absorption at 1940 nm ideally [19]. Although free-running Ho:YAG lasers are in clinical use, especially for fragmentation purposes, the cutting capabilities, either in cw or in Q-switched mode, are

not available [17,18,20]. Therefore, further experiments are needed to identify the potential of the technical possibilities of this innovative laser system. The observed reproducible and defined coagulation could potentially be an important factor for clinical use, e.g. precise non-contact laser-assisted preparation with defined thermal damage of the remaining tissue.

Conclusions

An innovative fan-cooled laser system in the 2 μm wavelength regime was developed which could be switched between pulsed and cw light emission mode as well as between different emission wavelengths. The fact that the ablation thermal effects on the remaining tissue are limited to 1 ± 0.5 mm is encouraging with regard to the potential for the laser-assisted preparation near to sensitive structures. The sealing capacity of the system as well as its potential for its use in the thermal occlusion of vessels must be investigated in perfused tissue models. Finally, further investigations are needed to identify the main application parameters and possible clinical application fields for these kinds of lasers.

Acknowledgement

The authors would like to thank the Russian Academy of Science and Russian Ministry of Education and Science for the financial support through the program "Nonlinear-optical methods and materials for novel laser systems" and contract No. 14.740.11.0071.

Zusammenfassung

Ex-vivo-Untersuchungen des Schneideffekts von zwei experimentellen IR-Lasersystemen (cw Tm:YLF, cw/ Q-switched Ho:YAG)

Hintergrund: IR-Laserstrahlung im 2 μm-Bereich wird gut von Wasser, der wichtigsten Gewebekomponente, absorbiert und kann gleichzeitig noch gut mittels Lichtwellenleiter vom Lasergerät zum Gewebe transportiert werden. Somit zeigt diese Strahlung ein hohes Potenzial sowohl für endoskopische als auch für offen chirurgische Interventionen. Kommerzielle medizinische Lasergeräte in diesem Wellenlängenbereich basieren technisch auf Blitzlampen- oder Laser-gepumpten gepulsten Ho:YAG-Systemen oder kontinuierlich abstrahlenden (cw) Thulium-dotierten Faserlasersystemen. Die vorliegende Arbeit untersucht die Laser-Gewebe-Wechselwirkung von zwei experimentellen IR-Lasersystemen (Dioden-gepumpter cw Tm:YLF-Laser, cw und Q-switched Ho:YAG-Laser) im *Ex-vivo*-Experiment.
Material und Methodik: Der Dioden-gepumpte, luftgekühlte Tm:YLF-Laser (IAP RAS Prototyp) emittiert Licht mit einer Wellenlänge von 1909 nm im cw-Betrieb mit einer Leistung von max. 20 W und einer Konversionseffizienz von über 40%. Der Ho:YAG-Laser (IAP RAS Prototyp) wird von dem Tm:YLF-Laser gepumpt und emittiert bei einer Wellenlänge von 2090 nm im kontinuierlichen (cw) oder Q-switched-Modus mit einer durchschnittlichen Leistung von 10 W. Die Strahlqualität beider Lasersysteme liegt bei $M^2 < 1{,}3$. Somit kann die Laserstrahlung einfach in Low-OH-Lichtwellenleiter eingekoppelt werden.
Die Laser-Gewebe-Wechselwirkung beider Systeme wurde *ex-vivo* an Nieren- und Lebergewebe vom Schwein untersucht. In einem standardisierten experimentellen Aufbau wurden sowohl Einzelspot- als auch Schneid-Experimente durchgeführt. Bei den Einzelspot-Experimenten betrug der Abstand zwischen Gewebeoberfläche und Lichtwellenleiterendfläche $d = 5$ mm, wohingegen die Schneid-Experimente im Kontakt ($d = 0$ mm) und mit einer konstanten linearen Bewegungsgeschwindigkeit des Lichtwellenleiters ($v = 1$ mm/s) durchgeführt wurden. Die applizierten Laserenergien lagen im Bereich von 10–200 J. Die Gewebeeffekte wurden makroskopisch vermessen und histologisch ausgewertet.
Ergebnisse: In den Experimenten zeigte sich eine präzise und reproduzierbare Ablation mit klar umschriebenem Koagulationssaum. Die Ablationstiefe war abhängig von der applizierten Laserenergie. Histologisch konnte eine konstante Ausdehnung der Koagulation in axialer und in radialer Richtung von $1 \pm 0{,}5$ mm ermittelt werden.
Zusammenfassung: Die vorgestellten Lasersysteme zeigen eine hohe Schneideffizienz. Die induzierten Gewebeeffekte (Ablation, Koagulation) sind reproduzierbar. Die reproduzierbar konstante und geringe Ausdehnung des Koagulationssaumes macht einen Einsatz für die lasergestützte präzise Gewebepräparation während chirurgischer Interventionen denkbar.

Schlüsselwörter: Laser-Chirurgie; IR-Laser; 2 μm-Bereich; Laser-Gewebe-Wechselwirkung; Tm:YLF-Laser; Ho:YAG-Laser

References

[1] Walsh BM. Review of Tm and Ho materials: spectroscopy and lasers. Laser Phys 2009;19(4):855–66.
[2] Scholle K, Lamrini S, Koopmann P, Fuhrberg P. 2 μm laser sources and their possible applications. In: Bishnu P, editor. Frontiers in guided wave optics and optoelectronics. Vucovar: INTECH Publishing; 2010. p. 471–500.
[3] Theisen-Kunde D, Tedsen S, Danicke V, Keller R, Brinkmann R. Laser-scalpel for kidney resection based on 1.94 μm fibre laser system. In: Buzug TM, Holz D, Bongartz J, Kohl-Bareis M, Hartmann U, Weber S, editors. Advances in Medical Engineering. Springer Proceedings in Physics, Vol. 114. Berlin, Heidelberg and New York: Springer; 2007. p. 431–4.
[4] Wenk S, Fürst S, Danicke V, Theisen-Kunde D. Design and technical concept of a Tm laser scalpel for clinical investigation based on a 60 W, 1.92 μm Tm fiber laser system. In: Buzug TM, Holz D, Bongartz J, Kohl-Bareis M, Hartmann U, Weber S, editors. Advances in Medical Engineering. Springer

Proceedings in Physics, Vol. 114. Berlin, Heidelberg and New York: Springer; 2007. p. 447–52.
[5] Fried NM. High-power laser vaporization of the canine prostate using a 110 W thulium fiber laser at 1.91 μm. Lasers Surg Med 2005;36(1):52–6.
[6] Yiu MK, Liu PL, Yiu TF, Chan AY. Clinical experience with holmium:YAG laser lithotripsy of ureteral calculi. Lasers Surg Med 1996;19(1):103–6.
[7] Minaev VP. Laser apparatus for surgery and force therapy based on high-power semiconductor and fibre lasers. Quantum Electron 2005;35(11):976–83.
[8] Honea EC, Beach RJ, Satton SB, Speth JA, Mitchell SC, Skidmore JA, et al. 115-W Tm:YAG diode-pumped solid-state laser. IEEE J Quantum Electron 1999;33(9):1592–9.
[9] Eichhorn M, Kieleck C, Hirth A. Q-switched Tm3+:YAG rod laser with crystalline fiber geometry. In: Conference on Lasers and Electro-Optics/International Quantum Electronics Conference, OSA Technical Digest (CD) (Optical Society of America), 2009; paper CWH2. <http://www.opticsinfobase.org/abstract.cfm?URI=CLEO-2009-CWH2>.
[10] Zakharov NG, Antipov OL, Savikin AP, Sharkov VV, Eremeikin ON, Frolov YN, et al. Efficient emission at 1908 nm in a diode-pumped Tm:YLF laser. Quantum Electron 2009;39(5):410–7.
[11] ISO 11146:1999 Lasers and laser-related equipment – Test methods for laser beam parameters – Beam widths, divergence angle and beam propagation factor.
[12] Zakharov NG, Antipov OL, Sharkov VV, Savikin AP. Efficient lasing at 2.1 μm in a Ho:YAG laser pumped by a Tm:YLF laser. Quantum Electron 2010;40(2):98–100.
[13] Duck FA, editor. Physical properties of tissue: a comprehensive reference book. London: Academic Press; 1990.
[14] Wieliczka DM, Weng S, Querry MR. Wedge shaped cell for highly absorbent liquids: infrared optical constants of water. Appl Opt 1989;28(9):1714–9.
[15] Bach T, Netsch C, Haecker A, Michel MS, Herrmann TR, Gross AJ. Thulium:YAG laser enucleation (VapoEnucleation) of the prostate: safety and durability during intermediate-term follow-up. World J Urol 2010;28(1):39–43.
[16] Stepp H, Sroka R. Possibilities of lasers within NOTES. Minim Invasive Ther Allied Technol 2010;19(5):274–80.
[17] Bader MJ, Tilki D, Gratzke C, Sroka R, Stief CG, Reich O. Ho:YAG-laser: treatment of vesicourethral structures after radical prostatectomy. World J Urol 2010;28(2):169–72.
[18] Aho TF, Gilling PJ. Current techniques for laser prostatectomy – PVP and HoLEP. Arch Esp Urol 2008;61(9):1005–13.
[19] Hale GM, Querry MR. Optical constants of water in the 200-nm to 200-microm wavelength region. Appl Opt 1973;12(3):555–63.
[20] Bader MJ, Gratzke C, Walther S, Weidlich P, Staehler M, Seitz M, et al. Efficacy of retrograde ureteropyeloscopic holmium laser lithotripsy for intrarenal calculi >2 cm. Urol Res 2010;38(5):397–402.